ELSEVIER

Journal of Power Sources 55 (1995) 73–79

JOURNAL OF POWER SOURCES

Degradation phenomena in the cathode of a solid oxide fuel cell with an alloy separator

S. Taniguchi, M. Kadowaki, H. Kawamura, T. Yasuo, Y. Akiyama, Y. Miyake, T. Saitoh

New Materials Research Center, SANYO Electric Co., Ltd., 1-1 Dainichi-higashimachi, Moriguchi City, Osaka 570, Japan

Received 26 October 1994; accepted 28 November 1994

Abstract

A study is made of the cathode degradation phenomena in a solid oxide fuel cell that uses an alloy separator. Under the action of the discharge current, chromium diffuses from the alloy to the cathode and moves to the cathode/electrolyte interface. The cathode polarization increases in correlation with the intensity of chromium at the cathode/electrolyte interface. The increase in cathode polarization by the discharge current is due to chromium filling the pores at the cathode/electrolyte interface. This restricts diffusion of oxygen gas and decreases the number of electrode reaction sites. Chromium displacement at the cathode/electrolyte interface appears to be caused by the decrease in oxygen activity at the cathode/electrolyte interface.

Keywords: Solid oxide fuel cells; Cathodes; Degradation

1. Introduction

Planar-type, solid oxide fuel cells (SOFCs) have received a great deal of attention because of their simple manufacturing process and the promise of a higher power density than that available from corresponding tubular designs.

For the separator material, a heat-resisting alloy must offer good performance in terms of electrical and heat conductivity, gas-tightness, mechanical strength, and ease of manufacturing. It has been pointed out, however, that chromium diffuses from the alloy to the cathode at the operating temperature of 1000 °C and degrades the properties of the electrode [1,2].

The authors have studied the effect of surface treatment of the alloy separator and found that heat treatment and polishing can reduce the amount of chromium that diffuses from the alloy. A 150 mm^2 single cell was operated for about 3000 h [3]. There exists, however, many phenomena that are not clearly understood. These include polarization increase with time by the discharge current, and chromium displacement to the cathode/electrolyte interface. This work examines such cathode degradation phenomena and considers the mechanism of chromium displacement to the cathode/electrolyte interface.

2. Experimental

The test cells were constructed as follows. The electrolyte was made from PSZ (3 mol% Y_2O_3 + 97 mol% ZrO_2) and the thickness was 200 μm. The anode material comprised NiO 1 μm, 56 wt.% + YSZ (i.e., 8 mol% Y_2O_3 + 92 mol% ZrO_2) 0.5 μm, 44 wt.% and was painted on the surface of the electrolyte. It was then sintered at 1250 °C for 2 h.

$La_{0.9}Sr_{0.1}MnO_3$ 1 μm, 80 wt.% + YSZ 0.5 μm, 20 wt.% was used for the cathode material, except in the 1100 °C cell test. $La_{0.7}Sr_{0.1}MnO_3$ 1 μm, 80 wt.% + YSZ 0.5 μm, 20 wt.% was used in this latter test because of its reduced reactivity with YSZ. The cathode material was painted on the other side and sintered at 1100 °C for 4 h. The reference electrode was on the cathode side. The current-collector was a platinum mesh. The thickness of each electrode and accompanying current-collector was about 100 μm.

In Section 3.1 the electrode size for the test cells was 4 mm × 12.5 mm. Alloy test pieces of Inconel 600 (16wt.%Cr–8wt.%Fe–76wt.%Ni) were made by a machining process. The size of these pieces was 2 mm × 2 mm × 12.5 mm. In order to evaluate the influence of chromium that diffuses from the alloy to the cathode, the test pieces were not given any surface treatment

SSDI 0378-7753(94)02172-Y

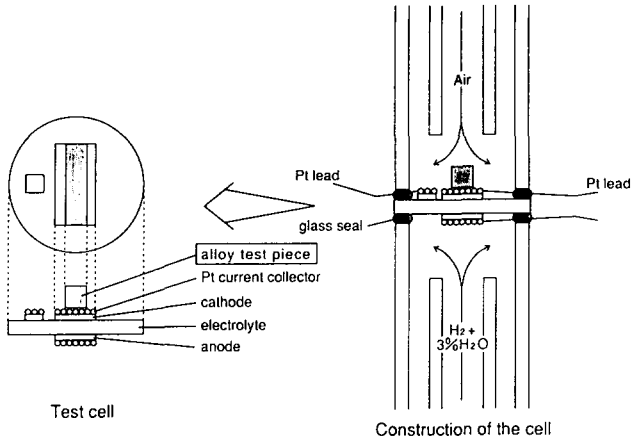

Fig. 1. Schematic of the design of the test cell.

and put on the cathode as shown in Fig. 1. Test cells were operated at 1000 °C with air (cathode) and $H_2+3\%$ H_2O (anode) gas.

In Section 3.2 the electrode had a diameter of 8 mm in the test cells. Oxide (Cr_2O_3, $NiCr_2O_4$, $CoCr_2O_4$, $LaCrO_3$) tablets were used instead of the alloy to keep the volatility of CrO_3 constant. The diameter of these tablets was 10 mm and they were press-formed and sintered at 1400 °C. These tablets were then placed on the cathode. Test cells were operated at various temperatures and oxygen vapour pressures in order to clarify the mechanism of chromium displacement at the cathode/electrolyte interface. The oxygen vapor pressure was controlled using O_2, air and N_2 gas.

Ohmic loss and polarization were measured by current-interruption method. The distribution of chromium in the cathode and the microstructure of the cathode were measured by electron probe microanalysis (EPMA) and scanning electron microscopy (SEM).

3. Results and discussion

3.1. Cathode degradation phenomena with untreated Inconel 600

Fig. 2 shows the change in cell voltage and cathode polarization with time. The cell voltage decreased after a few hundred hours. This deterioration was due to an increase in the cathode polarization.

Fig. 3 shows the change in cell voltage with time for two operating conditions, together with the chromium distribution in the cathode. The first condition (I) shows the cell performance tested with a constant current density of 0.3 A/cm² from the initial stage, and the second (II) indicates a cell tested with no current during an initial stage of 300 h and a constant-current density of 0.3 A/cm² applied after this period. The cell voltage (I) decreased with time from the beginning with increase in cathode polarization. After ~400 h (a), the cell

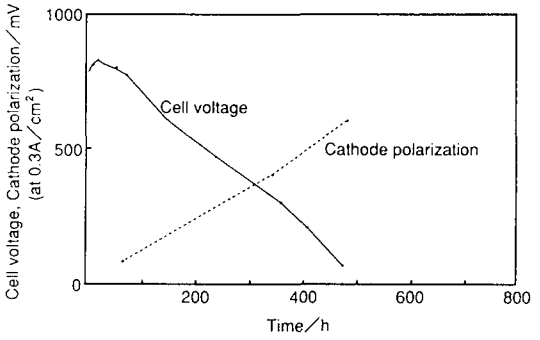

Fig. 2. Cell voltage and cathode polarization for a cell using untreated Inconel 600. The cell was operated at a constant-current density of 0.3 A/cm² at 1000 °C with $H_2+3\%$ H_2O (anode) gas and air (cathode).

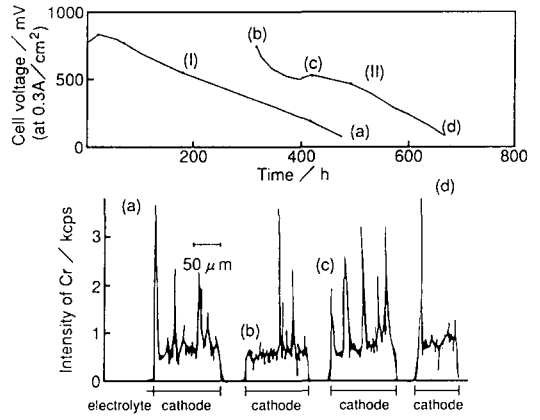

Fig. 3. Cell voltage for the following two operating conditions ((I) and (II)) and chromium distribution in the cathode at each time ((a), (b), (c) and (d)): (I) tested with a constant-current density of 0.3 A/cm² from the initial stage, and (II) tested with no current during the initial stage of 300 h and a constant-current density of 0.3 A/cm² applied after 300 h.

voltage had decreased from the initial ~700 to ~100 mV and the chromium distribution in the cathode was displaced to the cathode/electrolyte interface. On the other hand, the chromium distribution in cell (II) exhibited no displacement after 300 h (b), and a deterioration in cell performance deterioration was not observed. After the current was applied, however, the cell voltage (II) began to decline with the increase in cathode polarization. The intensity of chromium at the cathode/electrolyte interface increased almost at the same speed as (I), in correspondence with the increase in cathode polarization, (c) and (d). This suggested that cell performance degradation was not determined by the time at 1000 °C, but rather by the time that the discharge current was applied. Chromium was moved to the cathode/electrolyte interface by the discharge current, and the increase in polarization appeared to correlate with the intensity of chromium at this interface.

The relationship between the intensity of chromium at the cathode/electrolyte interface and the increase in cathode polarization for a 1000 °C air condition is presented in Fig. 4. Samples with various conditions (alloys, operating conditions) are plotted in Fig. 4. The open circles give the value just after the current was

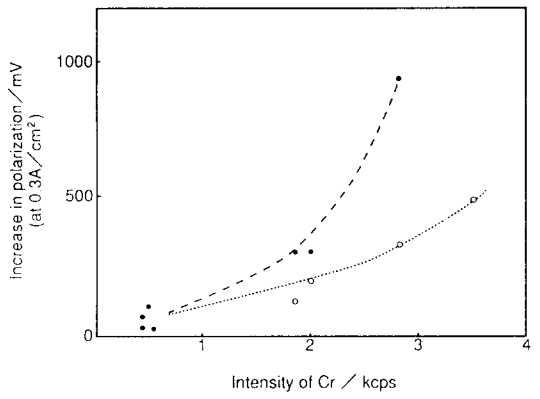

Fig. 4. Relationship between the intensity of chromium at the cathode/electrolyte interface and the increase in cathode polarization for a 1000 °C air condition: (○) value just after the current is applied, and (●) value 1 h later. EPMA measurement condition: 20 kV, 0.02 μA, crystal LiF(Cr).

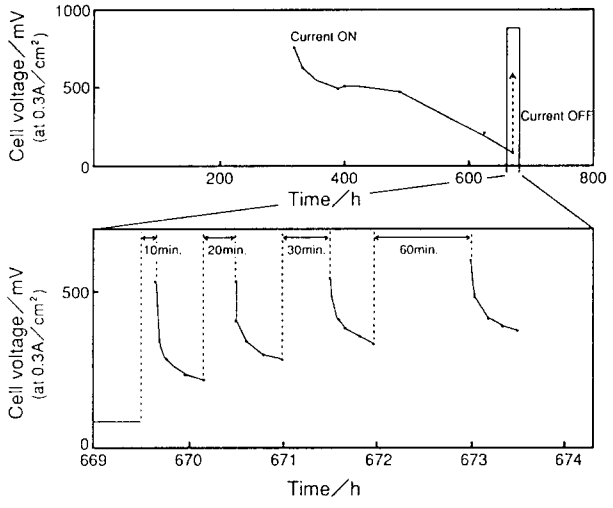

Fig. 5. Change in cell voltage for a cell with large polarization ((d) in Fig. 3) after interrupting the discharge current.

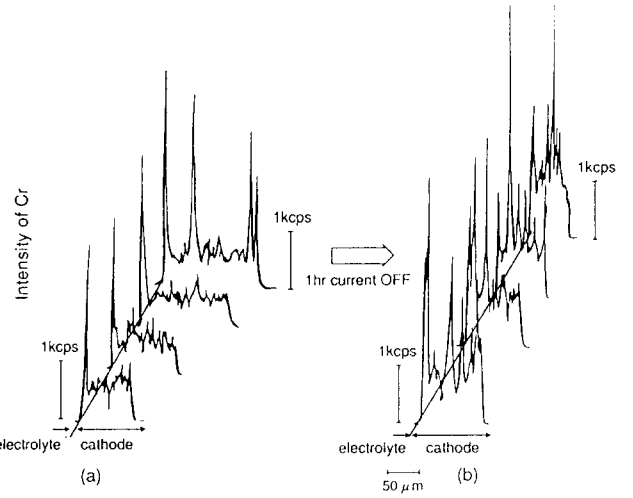

Fig. 6. Change in chromium distribution in the cathode by the interruption of the discharge current. Cell (a) had a large polarization and its temperature was lowered to room temperature while the discharge current was applied. Cell (b) had the same polarization as cell (a) and its temperature was lowered to room temperature after the discharge current was interrupted for 1 h. EPMA measurement condition: 20 kV, 0.02 μA, crystal LiF(Cr).

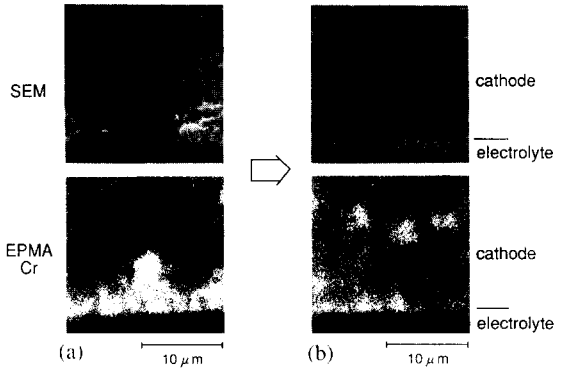

Fig. 7. Microstructure and chromium distribution in the cathode of the same samples used in Fig. 6.

applied and the closed circles indicate the value for 1 h later. When the intensity of chromium increased, polarization increased and the cell performance became unstable. With a high chromium content at the interface, the polarization increased from the time the current was applied.

Fig. 5 shows the change in cell voltage of a cell with large polarization ((d) in Fig. 3) after interrupting the discharge current. The cell voltage recovered from ~100 to ~600 mV after an interruption of 10 min. The cell voltage decreased with time, however, when a discharge current was applied. The cell voltage recovered to higher levels with longer interruption times.

Fig. 6 shows the change in chromium distribution in the cathode caused by the interruption of the discharge current. Cell (a) had large polarization and its temperature was lowered to room temperature while the discharge current was applied. Cell (b) had the same polarization as cell (a) and its temperature was lowered to room temperature after the discharge current was interrupted for 1 h. The chromium distribution in cell (a) showed a larger displacement to the cathode/electrolyte interface than in cell (b). Chromium was observed to diffuse to the electrode after the discharge current was interrupted (cell (b)). Fig. 7 shows the microstructure of the cathode and chromium distribution profile with the same sample used in Fig. 6. The pores are found to be filled with chromium at the cathode/electrolyte interface (see (a)), and there is diffusion of chromium to the electrode side when the discharge current was interrupted (cell (b)). The increase in polarization appears to be due to the chromium filling the pores and thus presenting diffusion of oxygen gas and decreasing the electrode reaction site.

Next, in order to consider this mechanism, the distribution of chromium in the cathode was studied. Fig. 8 shows the change in the chromium intensity over

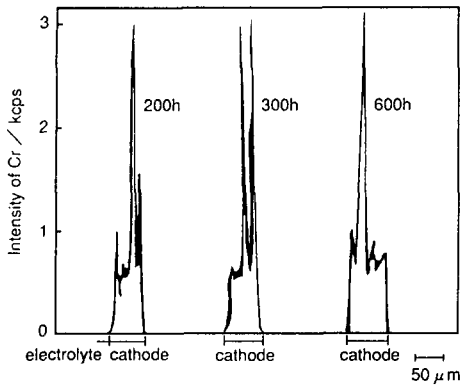

Fig. 8. Change in chromium intensity over time in the cathode without applying a discharge current. EPMA measurement condition: 20 kV, 0.02 μA, crystal LiF(Cr).

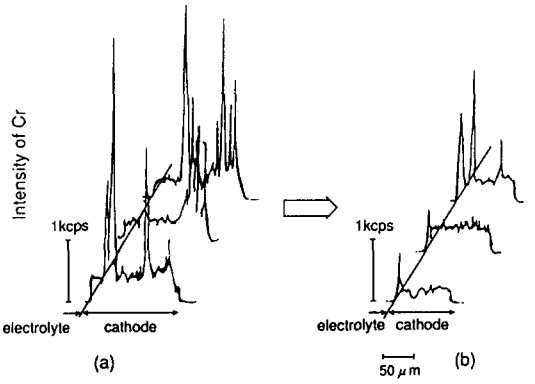

Fig. 9. Change in chromium distribution without an alloy on the cathode. (a) Sample left at 1000 °C with the alloy test piece on the cathode. (b) Sample prepared with the same conditions as (a) and then an alloy test piece was removed and the sample was used for the cell test for several hundred hours without the alloy. EPMA measurement condition: 20 kV, 0.02 μA, crystal LiF(Cr).

time in the cathode without applying a discharge current. There was little increase in the amount of chromium in the cathode with time. In Fig. 3, the fact was already discovered that the degradation in cell performance does not depend on the time at 1000 °C, but on the time that the discharge current was applied. These results indicate that the distribution of chromium in the cathode remains virtually constant when the cell discharge is not applied.

Fig. 9 presents the change in chromium distribution without an alloy on the cathode. The curves in (a) are for a sample that was left at 1000 °C with the alloy test piece on the cathode, while Fig. 9(b) refers to a sample that had been prepared with the same conditions as sample (a) and then the alloy test piece was removed and was used for the cell test for several hundred hours without the alloy. These was almost no deterioration in performance of sample (a); the cell voltage remained for a few hundred hours. In test (b), the chromium distribution was displaced to the cathode/electrolyte interface, but the intensity of chromium was decreased. This result indicates that a part of the chromium content was removed by the oxidant gas. Chromium diffusion appears to occur mainly in gas states. The vapor pressure of CrO_3 has the highest value of all the gaseous species containing chromium at 1000 °C in air. The vapor CrO_3 is considered to be produced at the surface of the alloy by the following reaction:

$$Cr_2O_3(s) + 1.5O_2(g) \longrightarrow 2CrO_3(g) \quad (1)$$

and is considered to exist in the cathode. The calculated vapor pressure of CrO_3 ($pCrO_3$) with MALT (materials-oriented little thermodynamic database for Personal Computers [4]) is 1.48×10^{-5} atm at 1000 °C in air. X-ray diffraction analysis revealed the presence of $(Mn,Cr)_3O_4$ in the cathode. This indicates that an exchange of manganese in $La_{0.9}Sr_{0.1}MnO_3$ and chromium takes place and $La_{0.9}Sr_{0.1}(Mn,Cr)O_3$ and $(Mn,Cr)_3O_4$ are formed. The CrO_3 vapor pressure in the cathode was kept constant by diffusion from the alloy. The intensity of chromium in the cathode appears to express the rate of reaction (1) and deposition of Cr_2O_3 at the surface of the electrode particles, i.e., the reverse of reaction (1).

Next, prior to the clarification of the chromium displacement process, an influence of current (not by cell discharge) was investigated. In Fig. 10, chromium distribution (by the current passed) from the cathode surface to the cathode/electrolyte interface by the platinum current-collector is presented. Although the direction of the current flow was the same as that of the cell discharge, the current had no influence on the chromium distribution. This result indicates that chromium displacement to the cathode/electrolyte interface is caused by the cathode electrode reaction.

3.2. *Clarification of the chromium-displacement process*

Fig. 11 shows the change in cell voltage with time for operating temperatures of 850, 900, 1000 and 1100 °C. Cr_2O_3 tablets were used instead of the alloy. The cell performance at the lower operating temperatures

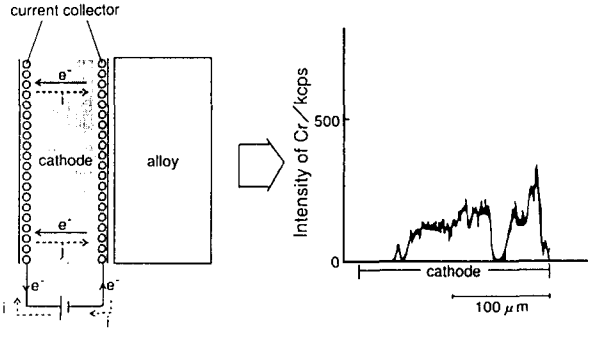

Fig. 10. Chromium distribution by the current passed from the cathode surface to the cathode/electrolyte interface by the platinum current-collector.

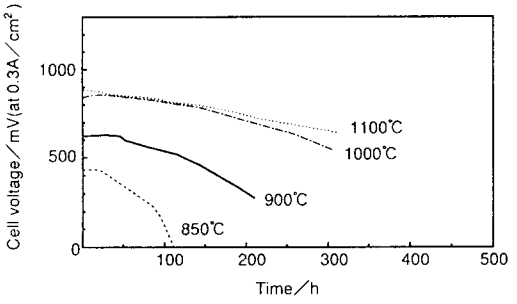

Fig. 11. Cell voltage for operating temperatures as shown, and with Cr_2O_3 tablets on the cathode. Each cell was operated at a constant-current density of 0.3 A/cm^2 with H_2+3% H_2O (anode) gas and air (cathode).

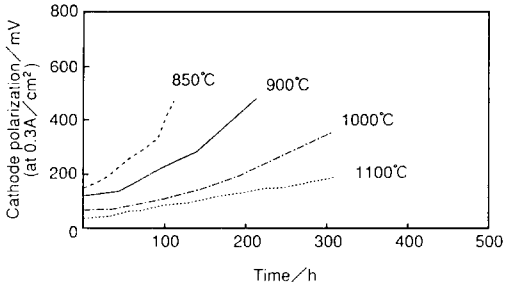

Fig. 12. Cathode polarization of cells itemized in Fig. 11.

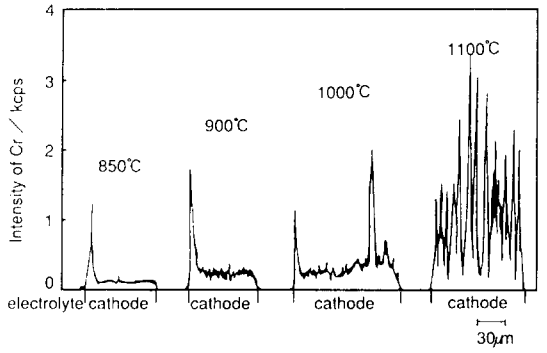

Fig. 13. Chromium distribution in the cathodes of cells itemized in Fig. 11. EPMA measurement condition: 20 kV, 0.02 μA, crystal LiF(Cr).

was inferior because of an increase in cathode polarization (Fig. 12). The chromium distribution in these cells is presented in Fig. 13. Although the average intensity was lower at lower operating temperatures, the displacement to the cathode/electrolyte interface was greater than at higher operating temperatures.

Fig. 14 presents the change in cell voltage over time at 900 °C for a cathode oxygen partial pressure of 1.0, 0.21 or 0.05 atm. In Fig. 14, the cell performance obtained in the absence of the alloy and in air is also presented. The cell performance did not change greatly with the oxygen partial pressure. The chromium distribution at higher oxygen partial pressures, however, exhibited a higher intensity at the cathode/electrolyte interface (Fig. 15). Cell performance cannot be determined only by the intensity of chromium at the interface because the changes in cathode electrode activity depend on the operating conditions.

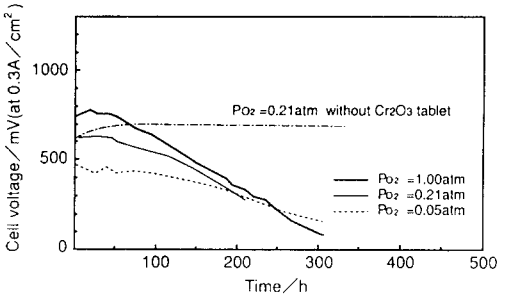

Fig. 14. Cell voltage for given partial pressures of cathode oxygen and with Cr_2O_3 tablets on the cathode. Each cell was operated at a constant-current density of 0.3 A/cm^2 at 900 °C with H_2+3% H_2O (anode) gas.

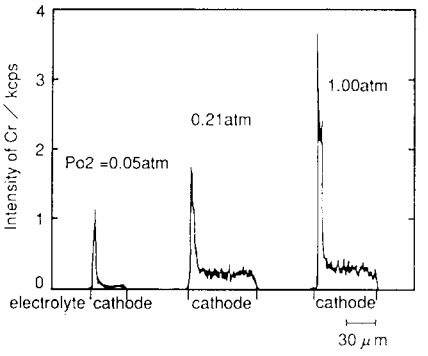

Fig. 15. Chromium distribution in the cathode of the cell Fig. 14. EPMA measurement condition: 20 kV, 0.02 μA, crystal LiF(Cr).

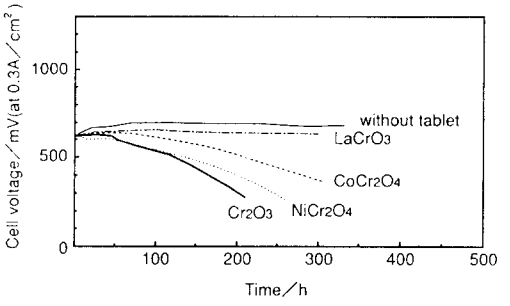

Fig. 16. Cell voltage for different CrO_3 vapor pressures. Each cell was operated at a constant-current density of 0.3 A/cm^2 at 900 °C with H_2+3% H_2O (anode) gas and air (cathode).

Fig. 16 gives the change in cell voltage over time at 900 °C for different CrO_3 vapor pressures. To change the CrO_3 vapor pressure, chromium oxide (Cr_2O_3, $NiCr_2O_4$, $CoCr_2O_4$, $LaCrO_3$) tablets were used; the vapor pressures were calculated with MALT [4]. They are listed in Table 1. In Fig. 16, the cell performance obtained in the absence of the alloys is also presented. The cell performance was affected by the CrO_3 vapor pressure and the intensity of chromium diminished with decreasing CrO_3 vapor pressure (Fig. 17).

Table 1
Calculated CrO_3 vapor pressure at various conditions

Oxide	Temperature (°C)	pO_2 (atm)	$pCrO_3$ (atm)
Cr_2O_3	1100	0.21	4.92×10^{-5}
Cr_2O_3	1000	0.21	1.48×10^{-5}
Cr_2O_3	900	1.00	1.20×10^{-5}
Cr_2O_3	900	0.21	3.73×10^{-6}
Cr_2O_3	900	0.05	1.27×10^{-6}
$NiCr_2O_4$	900	0.21	3.38×10^{-6}
$CoCr_2O_4$	900	0.21	1.34×10^{-6}
Cr_2O_3	850	0.21	1.70×10^{-6}

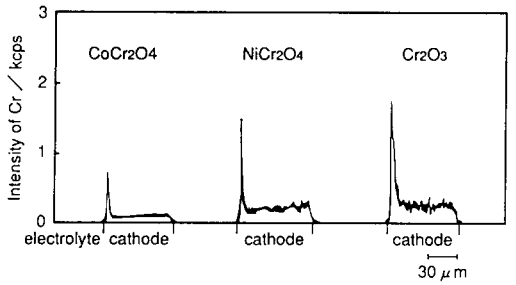

Fig. 17. Chromium distribution in the cathode of the cell in Fig. 16. EPMA measurement condition: 20 kV, 0.02 μA, crystal LiF(Cr).

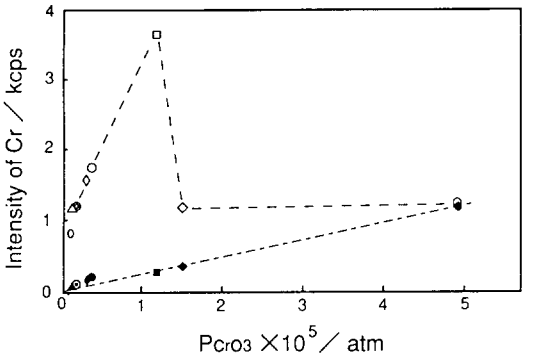

Fig. 18. Relationship between calculated CrO_3 vapor pressure and intensity of chromium in the cathode. The cell performance of each cell was shown in Figs. 11, 14 and 16. Open symbols are the intensity at the cathode/electrolyte interface and closed symbols indicate the average intensity in the cathode excluding the cathode/electrolyte interface. (◎)(⊙): 850 °C, $pO_2=0.21$ atm, Cr_2O_3; (0)(●): 900 °C, $pO_2=0.21$ atm, $CoCr_2O_4$; (◇)(◆): 900 °C, $pO_2=0.21$ atm, $NiCr_2O_4$; (△)(▲): 900 °C, $pO_2=0.05$ atm, Cr_2O_3; (○)(●): 900 °C, $pO_2=0.21$ atm, Cr_2O_3; (□)(■): 900 °C, $pO_2=1.00$ atm, Cr_2O_3; (◇)(◆): 1000 °C, $pO_2=0.21$ atm, Cr_2O_3; (○)(●): 1000 °C, $pO_2=0.21$ atm, Cr_2O_3.

In Fig. 18, the relationship between the calculated CrO_3 vapor pressure and the intensity of chromium in the cathode in the above data is presented. Open symbols give the intensity at the cathode/electrolyte interface and closed symbols indicate the average intensity in the cathode excluding the cathode/electrolyte interface. The average intensity is almost proportional to the calculated CrO_3 vapor pressure, but the intensity at the cathode/electrolyte interface appears to be influenced by another factor.

In Fig. 19, the ratio of the intensity of chromium at the cathode/electrolyte interface to the calculated CrO_3 vapor pressure is plotted versus the decrease in oxygen activity at the interface from the gas phase. The oxygen activity, a_0, was determined from the following equation:

$$a_0 = pO_2^{1/2} \exp(-2\eta F/RT) \quad (2)$$

The decrease in oxygen activity at the interface from the gas phase, $\Delta \log a_0$, was calculated from:

$$\Delta \log a_0 = -(2\eta F/RT) \log e \quad (3)$$

In these equations, pO_2 is the oxygen partial pressure in the cathode gas, and η is the cathode polarization. In Fig. 19, the cathode polarization at the beginning of the cell test (that is, the cell performance which was not affected by chromium) was adopted for η. The ratio of the intensity of chromium at the cathode/electrolyte interface to the calculated CrO_3 vapor pressure is closely related to the decrease in oxygen activity at the interface from the gas phase. This result indicates that chromium displacement is caused by the decrease in oxygen activity at the cathode/electrolyte interface by the cell discharge according to the following equation:

$$CrO_3(g) = 0.5Cr_2O_3(s) + 0.75O_2(g) \quad (4)$$

or

$$CrO_3(g) = 0.5Cr_2O_3(s) + 1.5O_{ad} \quad (5)$$

Here, O_{ad} is the adsorbed oxygen atom at the $La_{0.9}Sr_{0.1}MnO_3$ surface, and the intensity of chromium at the cathode/electrolyte interface is determined by both the CrO_3 vapor pressure and the decrease in oxygen activity at the interface from the gas phase. These processes are schematically illustrated in Fig. 20.

A rough estimation of the rate of the Cr_2O_3 deposition was made by the following method. The amount of O_2 that was consumed per 1 h in the cathode reaction:

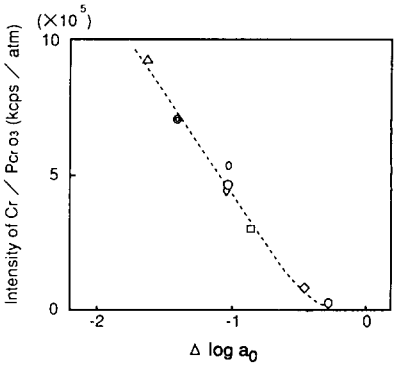

Fig. 19. Relationship between the ratio of the intensity of chromium at the cathode/electrolyte interface to the calculated CrO_3 vapor pressure and the decrease in oxygen activity at the interface from the gas phase.

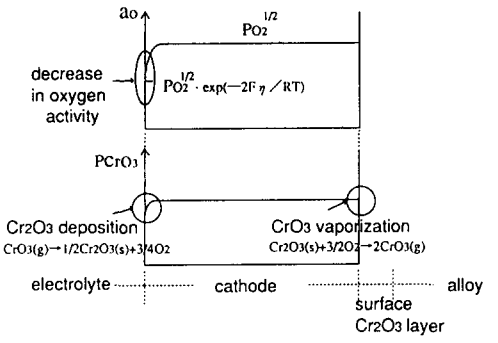

Fig. 20. Chromium vaporization and displacement process.

$$O_2 + 4e^- = 2O^{2-} \quad (6)$$

was:

$$i \times 60 \times 60/4F \text{ (mol/(cm}^2\text{ h))} \quad (7)$$

where $i = 0.3$ A/cm^2 is the current density. If it is assumed that $(3/4)(p(CrO_3)/pO_2)$ of the Cr_2O_3 was supplied in terms of the reverse Eqs. of (4) or (5), then the amount of Cr_2O_3 deposition at the interface would be:

$$(3/4)(pCrO_3/pO_2)(i \times 60 \times 60/4F) \times M(1/2)(4/3) \text{ (g/(cm}^2\text{ h))} = (pCrO_3/pO_2)0.215 \text{ (g/(cm}^2\text{ h))}$$

where $M = 153.2$ g mol is the Cr_2O_3 mass per 1 mol. Adopting a Cr_2O_3 volume of 0.192 cm^3/g, the thickness of the Cr_2O_3 deposit becomes

$$(pCrO_3/pO_2)0.0413 \text{ (cm/h)}.$$

In a 1000 °C/air condition, 2.90×10^{-6} cm/h or 2.90 μm per 100 h will be obtained.

If the exchange of manganese in $La_{0.9}Sr_{0.1}MnO_3$ and chromium and re-volatilization of the Cr_2O_3 deposit is combined, then the rate of Cr_2O_3 deposition at the cathode/electrolyte interface can be said to agree with the above estimation at 1000 °C air condition (Fig. 7(a)). Under other operating conditions, however, the rate of Cr_2O_3 deposition at the cathode/electrolyte interface varies due to the changes of $\Delta \log a_0$ at the interface, and the rate can be estimated only qualitatively.

4. Conclusions

Chromium that diffuses from the alloy to the cathode moves to the cathode/electrolyte interface by the discharge current, and cathode polarization increases in correlation with the intensity of chromium at the cathode/electrolyte interface. The increase in cathode polarization by the discharge current is due to chromium filling the pores. This hinders the supply of oxygen gas and decreases the number of cathode electrode reaction sites. It is concluded that chromium displacement at the cathode/electrolyte interface is caused by the decrease in oxygen activity at the cathode/electrolyte interface by the cell discharge.

Acknowledgements

This work was performed as an R&D program of the New Energy and Industrial Technology Development Organization (NEDO) under the New Sunshine Project of the Agency of Industrial Science and Technology, MITI.

References

[1] H. Koide, Y. Someya, T. Miyate and T. Yoshida, *Proc. 32th Battery Symp., Kyoto City, Japan, 17–19 Sept. 1991*, p. 209.

[2] S. Taniguchi, Y. Akiyama, N. Ishida, T. Yasuo, S. Murakami and T. Saitoh, *Proc. Autumn Meet., The Electrochemical Society of Japan, Sapporo City, Japan, 24–25 Sept. 1992*, p. 154.

[3] Y. Akiyama, S. Taniguchi, T. Yasuo, M. Kadowaki and T. Saitoh, *J. Power Sources, 50* (1994) 361.

[4] The Japan Society of Calorimetry and Thermal Analysis, *MALT, Materials-oriented Little Thermodynamic Database for Personal Computers*, 1985.